Effect of pH and Salt on the Adsorption and Interactions of an Amphoteric Polyelectrolyte

Yoichiro Kamiyama† **and Jacob Israelachvili***

Department of Chemical and Nuclear Engineering, University of California, Santa Barbara, California 93106

Received December 30, 1991; Revised Manuscript Received May 28, 1992

ABSTRACT: Adsorption and surface force measurements were carried out on gelatin (MW ~100 000) adsorbed on mica from aqueous NaCl solutions. Measurements were made over a range of ionic strengths and pH. The results show that gelatin adsorbs via discrete ionic bonds formed between negative surface groups on mica and positive basic groups on gelatin; these exist even when gelatin is *net* negatively charged (at a pH above the IEP of 5.0). The phenomenon of strong adsorption even when both the polymer and surface are net negatively charged does not appear to occur with macromolecules containing only acidic groups. The forces were generally repulsive: at separations beyond layer overlap the repulsion is dominated by an electrostatic "double-layer" force, while closer in it is dominated by a "brush-like" steric interaction. We discuss the effects of pH and salt on the configurations, the interaction forces, and the dynamics of the adsorbed coils.

Introduction

The adsorption of polymers onto solid surfaces from solution is important for understanding the interactions of colloidal particles and biological surfaces, the rheology of complex fluid systems, and the properties of thin films in general. The situation is particularly complex in the case of an amphoteric polyelectrolyte, a copolymer containing both basic and acidic groups: First, the polymer has both positive and negative groups which significantly complicates its segment–segment interactions. Second, its electrostatic interactions with a surface, which may also contain positive and negative groups, are also complex, as is the resulting force between two such polymer-covered surfaces. So far there have been no detailed experimental measurements or theories of the adsorption or interactions of such amphoteric polyelectrolytes. Such molecules are most commonly found as biological macromolecules, for example, as proteins (polypeptides), polynucleic acids, and gelatin. In this paper we report on our experiments with gelatin.

Gelatin is a denatured form of naturally obtained collagen and has been utilized since the very beginning of the photographic industry as a colloidal protective agent.[1-3] Even though in recent years a lot of progress has been made in the science of synthetic polymers, gelatin remains the sole ingredient for this purpose. Gelatin is a polypeptide copolymer consisting of both basic and acidic amino acid groups (i.e., gelatin is an amphoteric polyelectrolyte). Depending on whether the solution pH is above or below the isoelectric point (IEP) of gelatin, the molecule can be anionic, neutral, or cationic. However, it should be noted that both above and below the IEP the gelatin molecule simultaneously carries both negatively and positively charged groups.

Many studies have been made on the adsorption of gelatin, especially onto silver halide crystal surfaces, reflecting the practical interest in its photographic uses. In the 1960s, from results on the competitive adsorption of a cyanine dye, Curme and Natale[4] concluded that gelatin adsorbs onto silver bromide sol in loops and bridges, and that maximum adsorption occurs around the IEP.

From measured heats of adsorption, Berendsen and Borginon[5] concluded that the amount of gelatin adsorbed on AgBr is strongly pH-dependent, with the binding energy increasing at pH values below the IEP and remaining roughly constant above the IEP. Kragh and Peacock[6] investigated the adsorption and desorption isotherms of gelatin on AgBr both above and below the IEP and concluded that the adsorption was higher above the IEP than below the IEP, and also that a proportion of the gelatin was desorbable above the IEP.

Maternaghan et al.[7,8] conducted a detailed ellipsometric study of the effects of pH, pAg, electrolyte concentration, the lattice face of AgBr, degree of phthalation, and gelatin molecular weight on the adsorbed amount and adsorbed layer thickness. They concluded that over a wide range of experimental conditions gelatin molecules adsorb as a monolayer of random coils which are laterally compressed but otherwise only moderately deformed compared to their solution state, and that the adsorption excess reaches a maximum at the IEP except at very high salt concentrations.

As for surfaces other than silver halides, Kudish and Eirich[9] studied the adsorption on Pyrex and stainless steel surfaces. Around the IEP, the adsorption was maximum, and the area per adsorbed molecule was minimum. Recently, direct force measurements between gelatin layers adsorbed on mica from KCl solutions were reported by Kawanishi and Christenson.[10] They measured repulsive forces having a range of 50–100 nm from which they concluded that gelatin adsorbes both below and above the IEP, but that *minimum* adsorption occurs around the IEP.

In this study we investigated the adsorption and force–distance profiles of gelatin on mica, particularly as a function of electrolyte concentration, pH (above and below the IEP), and time.

Materials and Methods

All water used in these experiments was first treated with an ion exchange column, then distilled once in an all-Pyrex still, and finally passed through a Millipore water-purification system. After reaching equilibrium with the atmosphere, the water typically displayed a pH of 5.4–5.8 and an electrical conductivity of about 2 μS/cm. The NaCl used as the electrolyte and the HCl and NaOH used for adjusting the pH were of analar grade.

The gelatin was an inert bone gelatin of very low ion content, and of average molecular weight (~100 000) as estimated by gel permeation chromatography. Its properties are shown in Table I.

† On leave from Fuji Photo Film Co., Ltd., Tokyo, Japan.

0024-9297/92/2225-5081$03.00/0

Table I
Properties of Gelatin Used in Experiments

General Properties	
radius of gyration[a]	23 nm (pH 5.0, 10^{-1} M KCl)
isoelectric point[b]	pH 5.00 ± 0.05
gel strength[c]	231
viscosity[d]	63.2 mP
conductivity	14.4 μS/cm
moisture content	9.8%
Composition (Amino Acid Groups)[e]	
nonionic groups	
glycine, alanine, proline, valine, etc.	80%
anionic groups	
aspartic acid, glutamic acid, etc.	12%
cationic groups	
lysine, hydroxylysine, arginine, histidine, etc.	8%
ionic impurities	
Fe	1.4 ppm
Ca, Cu	0 ppm

[a] Estimate based on light scattering data of another gelatin (ref 4). [b] At the IEP, the net charge of gelatin is zero. The value of the IEP depends on the way gelatin is extracted from collagen (i.e., acid or lime processed) and on the duration of liming of the collagen stock. [c] Blooming in grams. Determined using a 6.7% w/v gel at 10 °C. [d] Determined using a 6.7% w/v gel at 40 °C. [e] The structure is as follows:

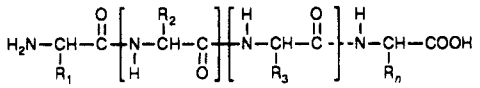

R_n = amino acid group ($n \approx 1000$)

All force measurements were carried out with a surface force apparatus (SFA) (Mk III).[11] Since many papers[12,13] have described the procedure of making force measurements with or without polymer, we will not repeat it here. All force runs were carried out at a gelatin concentration of 100 ppm at 25 °C.

The amount of gelatin adsorbed (the "adsorption excess") was measured independently using the microbalance technique developed by Terashima.[14,15] In this technique, the adsorption excess is obtained by directly measuring the mass of a mica sheet before and after it is submerged into a gelatin solution, i.e., first without and then with the adsorbed gelatin layer. Instead of the delicate torsion bar spring balance made of fused quartz originally used by Terashima et al.,[14,15] we used a commercial Mettler UM-3 microbalance[16] (readability 10^{-7} g, accuracy 10^{-6} g). Each weighing was conducted with two sheets of mica at a time in order to double the total surface area. The total exposed area of the mica sheets was 4×10^{-3} m^2, so that the accuracy in measuring the amount of polymer adsorbed is 0.25 mg/m^2. The merit of this direct weighing technique is that no complicated calculations nor complex theoretical assumptions are required to interpret the results.

The procedure for measuring the adsorption excess was as follows. First, the mass of a pair of cleaved mica sheets (approximately 30 mm wide × 34 mm long × 30 μm thick) was measured. Second, the sheets were washed in pure water, dried, and then weighed again. Those sheets were then immersed in a gelatin solution in a water bath for periods varying from 30 min to 16 h during which time the temperature was kept constant at 25 °C and the solution gently stirred by a magnetic stirrer. After retraction, the mica sheets were rinsed with a large excess of pure water by immersion (for 2 min) and finally dried and weighed again. The purpose of the water rinse was to wash out any unadsorbed gelatin and salt ions contained in the thin liquid film on the mica surface and in the pendant liquid droplet at the bottom edge of the mica sheet as it was withdrawn from the polymer solution. The pH of the rinsing water was adjusted to be the same as that of the gelatin solution where the adsorption took place. We have confirmed that 2 min of rinsing has a negligible effect on the mass of the adsorbed polymer under the conditions used here. All adsorptions were carried out under the same solution conditions as the subsequent force measurements, e.g., 100 ppm gelatin at 25 °C.

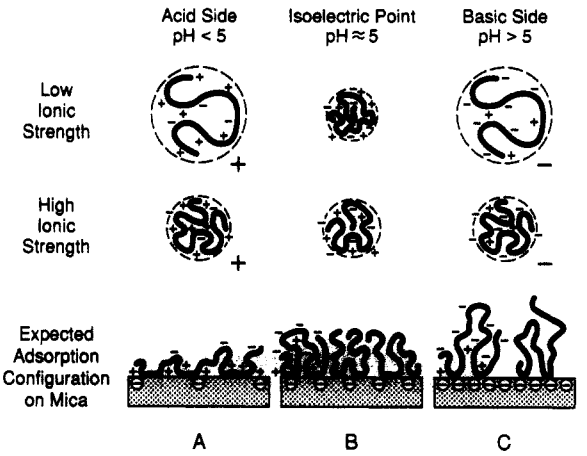

Figure 1. Likely coil configurations of gelatin in solution and when adsorbed onto a negatively charged (e.g., mica) surface as a function of pH and salt concentration.

Results and Analysis

Before describing the results, we would like to mention what is already known or expected about the configuration of gelatin molecules in solution and when adsorbed at a solid/liquid interface.

Expected Configurations below the Isoelectric Point (pH < 5.0). Below the IEP, gelatin molecules carry a net positive charge due to the dissociation of the amino groups. At low electrolyte concentrations (Figure 1A, top) the molecules are believed to be expanded due to the electrostatic repulsion between the positively charged segments. At high electrolyte concentrations (Figure 1A, middle) the coils become less expanded due to the increased screening of the electrostatic forces between the segments. In this pH regime the positively charged gelatin would be expected to strongly adsorb onto a negatively charged surface. More specifically, the positively charged amino groups should adsorb onto the negatively charged sites on mica (so long as the pH remains above ~3.0, the PZC of mica). This type of adsorption should lead to a relatively flattened configuration[4-6,8] (Figure 1A, bottom) which maximizes the number of positive charge contacts with the negatively charged surface sites.

Expected Configurations around the Isoelectric Point (pH ~5.0). In the region of the isoelectric point, interpretation of the phenomena is more difficult because the IEP is actually sensitive to the electrolyte concentration, falling to lower pH values in higher salt solutions.[3] When the net charge on the gelatin molecule is zero, one might expect the electrostatic repulsion between segments to vanish. However, in reality the charge is only zero on average, but may be highly positive or negative locally. At the IEP there is an equal number of oppositely charged groups which leads to an electrostatic *attraction* between the segments. The increased intersegment attraction is responsible for the reduced viscosity of gelatin at the IEP.[17] It also leads to a maximum in the segment density for coils both in solution and within the adsorbed layers (Figure 1B). The above effects also result in maximum adsorption at the IEP.[4,7-9]

Expected Configurations above the Isoelectric Point (pH > 5.0). Above the IEP, gelatin molecules carry a net negative charge due to the dissociation of the carboxyl groups. In this pH regime and at low electrolyte concentrations, gelatin molecules in solution are extended due to the electrostatic repulsion between the negatively charged segments (Figure 1C, top). As in the case below the IEP, the higher the electrolyte concentration the more condensed the configuration due to the increased screening

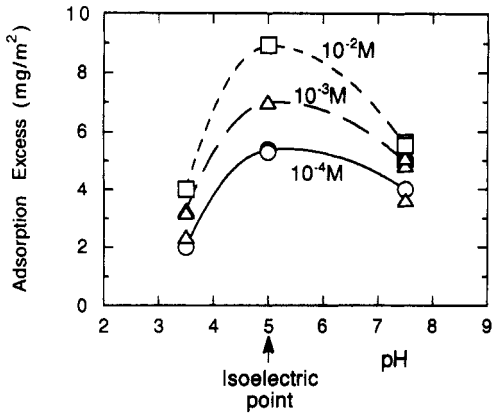

Figure 2. Measured adsorption of gelatin on mica as a function of solution pH and NaCl concentration using the direct weighing technique (refs 14–16).

of the electrostatic repulsion (Figure 1C, middle). However, above the IEP both gelatin and mica now have the same net (negative) charge, so that the electrostatic forces would appear to be unfavorable for adsorption. Yet several studies as well as ours have observed a reduced but still considerable adsorption of gelatin on mica. This could be due to (i) an electrostatic binding between the positively charged groups on gelatin and the negatively charged sites on mica or (ii) a short-ranged van der Waals or hydrophobic interaction between the undissociated groups on gelatin and the mica surface.[18] Either way, due to the high charge on the gelatin, the *longer-ranged* electrostatic repulsion between segments should result in less densely packed, or more extended, adsorbed layers[7,8,10] (Figure 1C, bottom).

Adsorption Measurements. Figure 2 shows the results of the adsorption excess experiments. The data shown were usually taken 2–5 h after commencement of adsorption. This was considered to be the equilibrium value since we did not observe any further increase after a further 16 h. Only at the IEP did the equilibrium time appear to be slightly greater than 2–5 h, and so a time of 5–7 h was allowed before the final measurements were made.

As shown in Figure 2, maximum adsorption occurred at the IEP, followed by the basic side of the IEP and then the acidic side. At any given pH, the adsorption generally increases with salt concentration. The maximum adsorption excess measured was about 9 mg/m^2. This corresponds to more than a monolayer even if the polymer is assumed to lie flat on the surface, which in turn suggests that the adsorbed coils contain many loops and extend well beyond the surface region, as illustrated in Figure 1B.

Force Measurements. Figure 3 shows the force profiles measured under nine different solution conditions ranging from pH 3.5 (1.5 pH units below the IEP) to pH 7.5 (2.5 pH units above the IEP), and from dilute 10^{-4} M to concentrated 10^{-2} M NaCl solutions. The DLVO forces before injection of polymer into the solution are shown by the dashed lines. These were dominated by exponentially repulsive electrostatic double-layer forces between the negatively charged mica surfaces. From the measured forces one could calculate the surface potential and charge: for example, in dilute 10^{-4} M NaCl (Figure 3A–C), the negative surface charge density increased from unit charge per 100 nm^2 at pH 3.5 to unit charge per 12 nm^2 at pH 7.5. This trend is as expected and also consistent with Pashley's earlier data on micas.[19] The nine surface potentials and charge densities are given in the legend to Figure 3.

After polymer was introduced into the chamber the forces were measured at various intervals up to 16 h after injection. Some of the force curves were highly reversible on approach (compression) and separation (decompression), and reproducible from one force run to the next and from one experiment to the next under the same conditions. These reversible force curves are shown by the black data points and continuous lines. Others were hysteretic and/or time dependent, where the initial force profile was different from the final, reversible force. These initial force profiles generally had a longer range than the final reversible forces, and they are shown by the white data points. They probably represent some initial, nonequilibrium state of the system, and the measured forces provide interesting insights into the kinetics of gelatin adsorption and the approach toward equilibrium under different solution conditions.

Before we describe the measured forces in detail, we first note some general features: (1) The forces are repulsive over the whole distance regime with a range between 1.5 and 4 R_g. (2) The tail end of each force curve is roughly exponential, with a decay length close to the Debye length. This shows that two approaching polymer-coated surfaces initially interact via a double-layer repulsion, with the outer Helmholtz plane (OHP, the plane of charge) effectively located somewhere within the polymer layer. (3) In high salt (short Debye lengths) where the double-layer force contribution is least, the range of the force is expected to reflect the thickness of the adsorbed polymer layers. Accordingly, Figure 3 indicates that the thinnest layers occur at pH 3.5, which is also the pH at which the adsorption was least. While the layer thickness and adsorption excess are strictly two separate quantities, that there is some correlation between the two is manifest when we compare the range of the forces of Figure 3 with the adsorption measurements of Figure 2. (4) Closer in, most of the force curves have a profile characteristic of the steric interaction between two adsorbed or end-grafted polymer layers, viz., a sharp initial rise from zero force (after subtraction of the double-layer force), followed by a flatter region, and then a sharp upturn in the force as the surface separation approaches zero (the "osmotic limit"). This suggests that once the polymer layers begin to overlap and become compressed, the interaction effectively goes from being electrostatically-dominated to sterically-dominated, a result that has been theoretically predicted by Pincus et al.[20,21]

Steric Forces. While there is no reason to expect two adsorbed polyelectrolyte layers to interact as two brush layers, we have found that the Alexander-de Gennes equation for the repulsive force between two polymer brush layers describes the steric part of the measured forces very well, both qualitatively and quantitatively (see below). Since the Alexander-de Gennes equation is very simple, and since it predicts force profiles that are anyway not very different from those expected for adsorbed layers,[22] we use it in our analysis of the results.

Once two brush-bearing planar surfaces are closer than twice the brush-layer thickness ($2L$) to each other the repulsive pressure between them is given by[23]

$$P(D) \approx (kT/s^3)[(2L/D)^{9/4} - (D/2L)^{3/4}] \qquad (1)$$

In order to get the force–distance ($F(D)$) relationship between two curved cylindrical surfaces, each of radius R, we first integrate eq 1 to obtain $W(D)$ and then use the

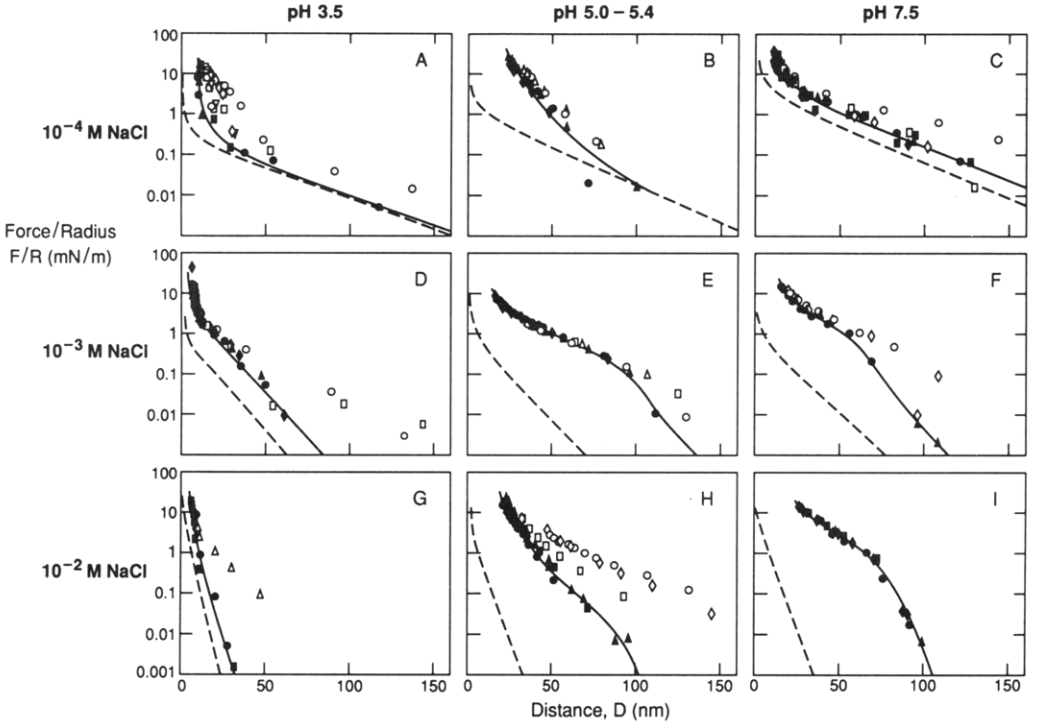

Figure 3. Measured forces F (normalized by the radius R of the surfaces) as a function of separation D between the mica surfaces. Dashed lines: forces in pure salt solutions before addition of polymer [surface potentials ψ_o and corresponding surface charge densities σ (nm^2 per unit charge) were as follows: A, $\psi_o = -31$ mV, $\sigma = 105$ nm^2; B, $\psi_o = -65$ mV, $\sigma = 58$ nm^2; C, $\psi_o = -180$ mV, $\sigma = 6.5$ nm^2; D, $\psi_o = -30$ mV, $\sigma = 59$ nm^2; E, $\psi_o = -40$ mV, $\sigma = 50$ nm^2; F, $\psi_o = -45$ mV, $\sigma = 48$ nm^2; G, $\psi_o = -60$ mV, $\sigma = 8.6$ nm^2; H, $\psi_o = -70$ mV, $\sigma = 9.4$ nm^2; I, $\psi_o = -90$ mV, $\sigma = 6.1$ nm^2]. White points: forces between adsorbed polymer layers measured 2–48 h after injection of polymer into the apparatus chamber. Black points and solid lines: final equilibrium (reversible) forces.

Derjaguin approximation[24] to obtain $F(D)$:

$$F(D) = 2\pi R W(D) = 2\pi R \int P(D)\, dD = (16\pi kTL/35s^3)[7(2L/D)^{5/4} + 5(D/2L)^{7/4} - 12] \quad (2)$$

As an example, we should be able to apply eq 2 to the case of Figure 3I where the interaction is expected to be dominated by steric forces since the high salt screens out most of the electrostatic contribution. Experimentally, too, little or no hysteresis was observed in the high pH solutions (for reasons that will be discussed later). Now, from Figure 2, the measured adsorption excess of gelatin in 10^{-2} M NaCl at pH 7.5 is 5.5 mg/m^2. Assuming a molecular weight of 100 000, the area occupied by one adsorbed gelatin molecule is therefore 30.2 nm^2, which corresponds to a mean distance between gelatin molecules of $s \approx 5.5$ nm. From the force measurements, we also know that the distance where the steric force starts is 95 nm, so that we may put $2L = 95$ nm. By substituting these values for s and L into eq 2, we obtain the force curve shown by the dashed line in Figure 4A.

The agreement between the "theoretical" and experimental results is surprisingly good. Note, however, that since eq 1 is derived from scaling theory, there is room to adjust the prefactor, which is unknown. We found that a prefactor of 1/3.5 (corresponding to a value of $s = 8$ nm, which is about 50% higher than the "measured" value) makes the theoretial curve coincide with the experimental points (Figure 4A, solid line). Figure 4B shows the likely configuration of the coils in solution and after being adsorbed on the negatively charged mica surfaces, as ascertained from the adsorption and force measurements.

Electrostatic Repulsion. It is difficult and perhaps impossible to separate the steric and electrostatic contributions to the net interaction in general. However, we have found that all the measured forces can be fitted by a steric brush-type repulsion in the overlap region together with a double-layer repulsion farther out. As an example, Figure 5A shows the measured equilibrium interaction at

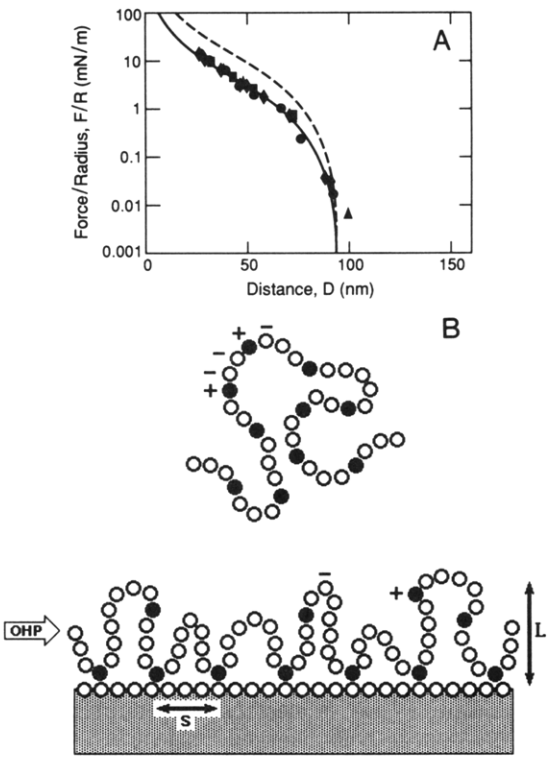

Figure 4. (A) Data points: measured forces in concentrated salt solutions (10^{-2} M NaCl, pH 7.5, detailed results of Figure 3). Solid line: theoretical brush repulsion based on eq 2 using $s = 8$ nm, $2L = 95$ nm, and $T = 25$ °C. (B) Likely configuration of polymer in solution and on the mica surface (schematic). The arrow indicates the possible location of the outer Helmholtz plane (OHP).

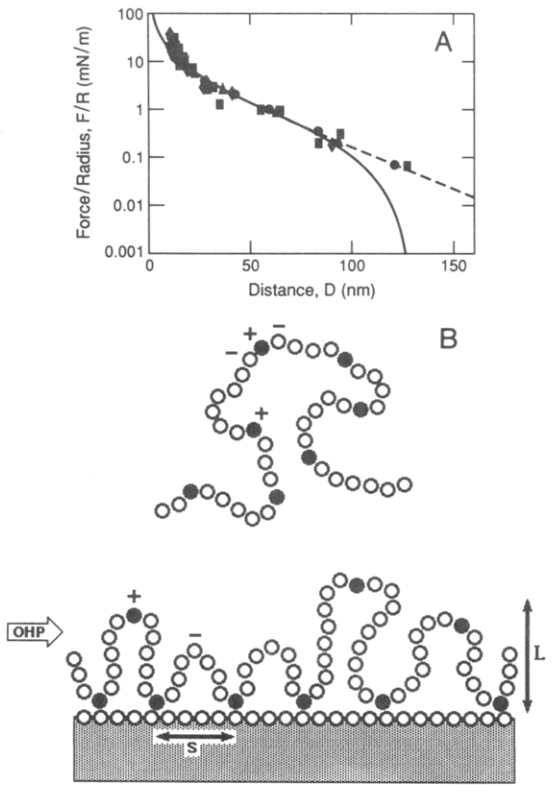

Figure 5. (A) Data points: measured forces in dilute salt solutions (10^{-4} M NaCl, pH 7.5, detailed results of Figure 3). Solid line: theoretical "charged brush" repulsion based on eq 2 using s = 14 nm and $2L$ = 120 nm (dashed line) together with an electrostatic double-layer tail of exponential decay length equal to the theoretical Debye length of 31 nm. (B) Likely configuration of polymer in solution and on the mica surface (schematic).

pH 7.5 (the same pH as in Figure 4A) but at a lower salt concentration of 10^{-4} M NaCl (cf. Figure 3C). The Debye length is now about 31 nm so that the electrostatic double-layer repulsion is no longer screened, and indeed the tail end of the interaction shows an exponential decay (dashed line) characteristic of the double-layer force in 10^{-4} M monovalent salt solutions. This electrostatic contribution was absent, or much suppressed, in high salt (cf. Figure 4A).

Figure 5A also shows the best fit theoretical curve to the data which consists of a brush-type repulsion close in (solid line) and an exponentially decaying double-layer repulsion farther out. The agreement between "theory" and experiment is again surprisingly good. However, it is worth pointing out that good agreement could be obtained over a range of values for s and L since one may now also adjust the magnitude of the double-layer contribution. Thus, reasonably good fits could be obtained over the range from s = 10 nm with $2L$ = 100 nm to s = 16 nm with $2L$ = 140 nm.

Effect of Salt. We may note that the fitted parameters for s and L in *low* salt (Figure 5A) are both slightly higher but similar to those obtained in *high* salt (Figure 4A). This is to be expected: in low salt the electrostatic repulsion between the segments is longer-ranged so that both the coil dimensions and layer thickness are expected to be more enhanced. Figure 5B shows the likely configuration of the coils in 10^{-4} M NaCl at pH 7.5, which may be compared with that in high salt (Figure 4B). The differences are not large, and manifest themselves mainly in a longer-ranged double-layer repulsion as the salt concentration is decreased.

Since the fitted parameters for s and L are similar in both high and low salt (as well as at the intermediate salt concentration of 10^{-3} M NaCl), we may tentatively conclude that salt plays a secondary role in the *adsorption excess* of gelatin layers, even though it has a large effect on the tail end of the *interaction* potential. Below we find that this conclusion also appears to hold at the other pH values studied.

Effect of pH: Below the IEP. pH had a much more dramatic effect than ionic strength, both on the adsorption and interactions of gelatin. Figure 6 shows the *reversible* force curves of Figure 3 (black points) together with the best fit theoretical plots based on the Alexander-de Gennes equation (solid lines) and an asymptotic double-layer tail (dashed lines). As can be seen from the fitted values of s and L, these vary greatly from one pH to the next, but only slightly on changing the salt concentration at the same pH. We now consider the interactions below the IEP, at the IEP, and above the IEP in turn.

At pH 3.5 (Figure 6A,D,G) there is only a small difference in the forces in the absence and presence of polymer. This suggests that the amount of polymer adsorbed is low and/or that the adsorbed molecules are in a flattened configuration. The measured forces therefore suggest that at pH 3.5 the coil configurations are as shown in Figure 7A. The coil in solution is expanded, very much as at high pH (Figure 7C), but the state of the adsorbed polymer is very different at pH 3.5: the mica surface is close to its PZC of 3.0, and there are much fewer negative sites for the polymer to bind to. Thus, despite the opposite net charges of the polymer and surface below the IEP of gelatin, the adsorbed amount is actually less and that above the IEP (where the polymer and surface have the same net charge and might have been expected to repel each other). This unexpected conclusion is consistent with the independent adsorption measurements shown in Figure 2; its implications are explored further in the Discussion. In addition, unlike at high pH where most of the polymer segments are repelled from the surface, thereby leading to a thick, expanded layer, at low pH there is no such repulsion, and so the chains can lie much closer to the surface.

At the IEP. At the IEP the force data can again be fitted (but not so well here) by a brush plus asymptotic electrostatic contribution as shown in Figure 6B,E,H. Again the effect of salt is mainly to modulate the tail end of the interaction potential but not the adsorption properties of the polymer itself. The forces indicate that the configuration of the adsorbed coils is as shown in Figure 7B, which is also consistent with the maximum in the absorption excess measured at the IEP (Figure 2). This maximum may be due to one or both of the following: (1) The equal number of positive and negative groups at the IEP means that the segments attract each other in solution and within the adsorbed layer. This condensed configuration favors a higher adsorption density. (2) At pH 5.0 mica is now more than 2 pH units above its PZC and the surface has a reasonably high concentration of negative sites.[25] Since the polymer also has a high density (50%) of positive groups, we find that this is the pH at which a large number of ionic bonds can form between positive and negative groups (even though the polymer is net neutral). The above two reasons probably account for why at the IEP of gelatin the adsorption excess is maximum and the adsorbed configuration is highly condensed.

Above the IEP. The force measurements (Figure 6C,F,I) confirm the results of the adsorption studies that showed significant adsorption of negatively charged gelatin on the negatively charged mica surfaces. This probably arises because of the still significant number of positive groups present on gelatin at pH 7.5 and the large number

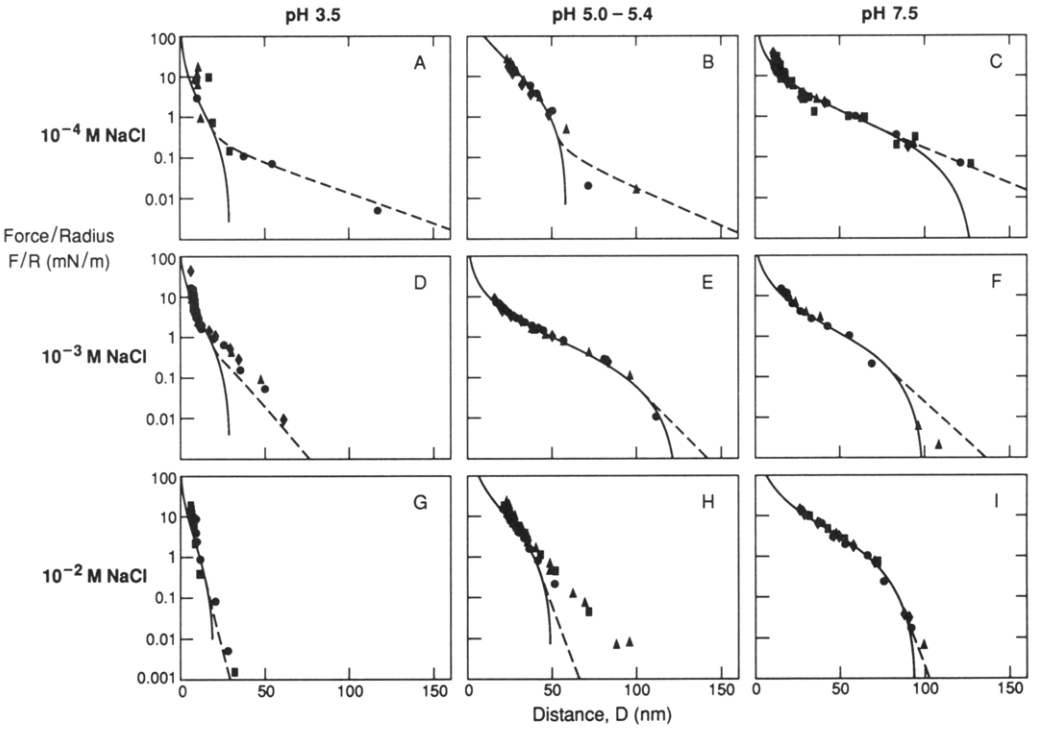

Figure 6. Equilibrium force curves of all nine equilibrium curves of Figure 3 together with the best fit theoretical plots on the Alexander-de Gennes equation (solid lines) and an asymptotic double-layer tail (dashed lines). The fitted values were as follows: A, s = 8 nm, $2L$ = 30 nm; B, s = 4.5 nm, $2L$ = 60 nm; C, s = 15 nm, $2L$ = 130 nm; D, s = 7 nm, $2L$ = 30 nm; E, s = 16 nm, $2L$ = 125 nm; F, s = 12 nm, $2L$ = 100 nm; G, s = 6 nm, $2L$ = 20 nm; G, s = 5 nm, $2L$ = 50 nm; I, s = 8 nm, $2L$ = 95 nm.

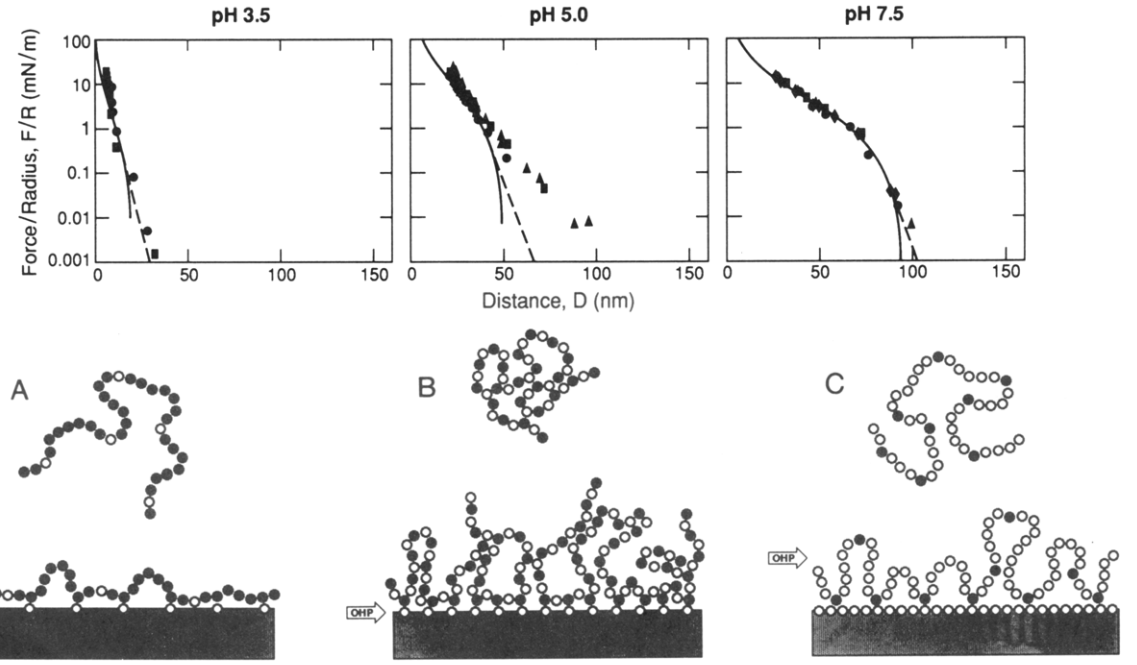

Figure 7. Top: Measured forces as a function of pH below and above the IEP (all at 10^{-2} M NaCl) together with the best fit theoretical plots based on the Alexander-de Gennes equation (solid lines) and an asymptotic double-layer tail (dashed lines). Bottom: Likely configurations of adsorbed polymers below and above the IEP.

of negative sites on the mica that they can bind to. This is shown schematically in Figure 7C. The high L values, indicative of expanded layers, are probably due to the large electrostatic segment–segment and segment–surface repulsions, which only occur at high pH.

Time-Dependent Effects. As can be seen from Figure 3, at high pH the forces were fairly reversible and the equilibrium times were fast. At the IEP and also at low pH the times to reach adsorption equilibrium were much longer (>2 h), and the forces were more hysteretic. These findings can be rationalized by considering the different conformations of the adsorbed coils at high and low pH. As illustrated in Figure 7C, at high pH the binding sites are spaced well apart from each other and the coils are well extended both from the surfaces and from each other; i.e., there are few entanglements. Both these factors are conducive to rapid equilibration. In contrast, at the IEP the coils are highly entangled with each other due to the high density of attractive ionic bonds between the segments (Figure 7B), while at low pH the strong binding of the segments to the surfaces gives rise to an effective "two-dimensional" entanglement of the flattened coils on the

surfaces (Figure 7A). Both of these effects are expected to reduce the adsorption and equilibration rates, as was observed, though at present there is no dynamic theory that can be applied to quantitatively test this hypothesis.

Discussion and Conclusions

Adsorption Mechanism of Amphoteric Polymers. Significant adsorption of gelatin on mica was measured even when both the polymer and the surfaces had the same net (negative) charge. This is in contrast to the absence of any adsorption of negatively charged PS-sulfonate[13,26] and SDS surfactants[27] on negatively charged mica surfaces. It is unlikely that van der Waals or hydrophobic interactions can be responsible for the adsorption: nonionic surfactants such as $C_{12}EO_5$ do not adsorb on mica. On the other hand, zwitterionic surfactants whose headgroups are net neutral but contain a positive–negative ion pair (a dipole or "zwitterion") bind very strongly to mica.[28,29] All this suggests that the adsorption of an amphoteric polyelectrolyte depends on the number of *discrete* ionic bonds that can be formed between the individual positively and negatively charged groups on the polymer and surface. In other words, the adsorption is determined by the details of the charge *distribution* and not by the average charge carried by the polymer and surface. This conclusion also shows that the adsorption depends on short-range electrostatic (Coulombic) interactions rather than long-range or continuum-type interactions. However, the net or average charge does determine the asymptotic long-range force between the polymer-bearing surfaces (see below).

Forces. The forces can be split into two effectively additive contributions: a steric brush-like repulsion at separations less than $2L$ (where L is the adsorbed layer thickness) and an electrostatic double-layer repulsion at separations greater than $2L$. We may refer to this simple model as the "charged brush" model, which has some theoretical justification (see ref 20 which shows that once two charged polyelectrolyte layers overlap electrostatic forces have only a minor effect on the overall interaction once the osmotic contribution of the trapped counterions is included). Thus, in the overlap regime ($D < 2L$) the forces are determined by the adsorption excess and the configuration of the adsorbed coils, which in turn depends mainly on the pH and less so on the salt concentration. However, at large separations ($D > 2L$), the repulsion finally decays exponentially as determined by the Debye length, which now depends more on the salt concentration than on the pH.

Dynamics of Adsorbed Coils. On the basic side of the IEP adsorption equilibrium was attained quickly, and the forces were always reversible (nonhysteretic). The much slower equilibration and relaxation times observed at the IEP and at lower pH are probably related to the coil entanglements that arise from the high density of segment–segment and segment–surface ionic bonds under these conditions. Figure 8 shows details of typical hysteretic forces measured at low pH and the likely coil configurations that lead to such effects; the latter is conceptually the same as the model previously proposed by Klein et al.[30] to explain hysteresis effects in the interactions of poly-L-lysine-bearing surfaces.

Comparison with Previous Experiments. Our results are consistent with the adsorption studies of Curme and Natale[4] and Kragh and Peacock[6] and the heat of adsorption measurements of Berendsen and Borginon[5] who first brought attention to the fact that gelatin adsorbs to negatively charged surfaces both below and above its IEP, and that maximum adsorption occurs at the IEP. Our results are also in agreement with the conclusions of Maternaghan et al.[7,8] and Kawanishi et al.[10] that gelatin adsorbs in a flattened configuration below the IEP, but in a much more expanded state above the IEP.

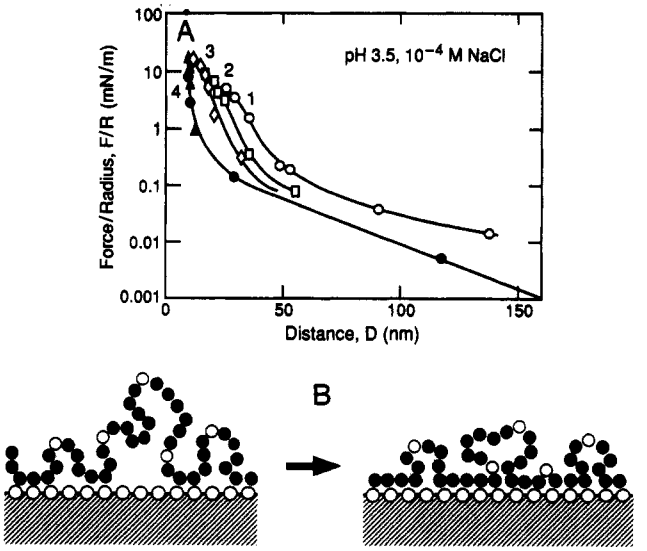

Figure 8. (A) Hysteretic forces measured at pH 3.5 and 10^{-4} M NaCl. Numbers refer to order in which forces were measured on approach and separation. Solid line: final reversible force. (B) Likely polymer configuration.

Concerning the forces, conformations, and hysteresis (or time-dependent effects) of adsorbed gelatin layers or even of other amphoteric polymer layers, there is little quantitative data to compare with. Gelatin is a good steric stabilizer of colloidal particles, but it can also cause bridging flocculation.[1] In addition, colloidal systems containing gelatin exhibit long relaxation times, especially when close to the IEP.[6,8] All of these effects would be consistent with our findings. Our various models for the coil conformations of gelatin in solution and when adsorbed to surfaces (Figures 1, 4B, 5B, 7, and 8B) may be somewhat speculative, but they are fully consistent with previous light scattering and viscosity measurements[31] as well as with the adsorption and force results reported here.

Acknowledgment. We thank Hiroshi Terashima for helpfully introducing us to his polymer adsorption measuring technique, and Jacob Klein, Yitzhak Rabin, and Phil Pincus for useful discussions.

References and Notes

(1) Ward, A. G.; Courts, A. *The Science and Technology of Gelatin*; Academic Press: London and New York, 1977.
(2) Cox, R. J. *Photographic Gelatin*; Academic Press: London and New York, 1972.
(3) Veis, A. *The Macromolecular Chemistry of Gelatin*; Academic Press: New York, 1964.
(4) Curme, H. G.; Natale, C. C. *J. Phys. Chem.* **1964**, *68*, 3009.
(5) Berendsen, R.; Borginon, H. *J. Photogr. Sci.* **1968**, *16*, 194.
(6) Kragh, A. M.; Peacock, R. *J. Photogr. Sci.* **1967**, *15*, 220.
(7) Maternaghan, T. J.; Bangham, O. B.; Ottewill, R. H. *J. Photogr. Sci.* **1980**, *28*, 1.
(8) Maternaghan, T. J.; Ottewill, R. H. *J. Photogr. Sci.* **1974**, *22*, 279.
(9) Kudish, A. T.; Eirich, F. R. *Proteins at Interfaces*; American Chemical Society: Washington, DC, 1987; p 261.
(10) Kawanishi, N.; Christenson, H.; Ninham, B. *J. Phys. Chem.* **1990**, *94*, 4611.
(11) Israelachvili, J. N.; McGuiggan, P. M. *J. Mater. Res.* **1990**, *10*, 2223.
(12) Israelachvili, J. N. *Intermolecular and Surface Forces*, 2nd ed.; Academic Press: London, 1991.

(13) Patel, S. S.; Tirrell, M. *Annu. Rev. Phys. Chem.* **1989**, *40*, 597.
(14) Terashima, H. *J. Colloid Interface Sci.* **1987**, *117*, 523.
(15) Terashima, H. *J. Colloid Interface Sci.* **1988**, *125*, 444.
(16) Terashima, H.; Kanehashi, K.; Imai, N. *Proceedings of the 1991 Materials Research Society meeting*, in press.
(17) Stainsby, G. In *The Science and Technology of Gelatin*; Ward, A. G., Courts, A., Eds.; Academic Press: London and New York, 1977; pp 109–136.
(18) It is worth pointing out that, at least theoretically, the van der Waals attraction is always expected to dominate at sufficiently small separations.
(19) Pashley, R. M. *J. Colloid Interface Sci.* **1981**, *83*, 531.
(20) Pincus, P. *Macromolecules* **1990**, *24*, 2912.
(21) Ross, R.; Pincus, P. *Macromolecules* **1992**, *25*, 2177.
(22) Luckham, P. F.; Klein, J. *J. Chem. Soc., Faraday Trans.* **1990**, *86*, 1363.
(23) de Gennes, P. G. *C. R. Acad. Sci., Ser. 2* **1985**, *300*, 839.
(24) Derajaguin, B. V. *Kolloid-Z.* **1934**, *69*, 155.
(25) Claesson, P. M.; Herder, P.; Stenius, P.; Eriksson, J. C.; Pashley, R. M. *J. Colloid Interface Sci.* **1985**, *109*, 31.
(26) Matthew Tirrell, private communication.
(27) We have observed only extremely small or no adsorption of nonionic or anionic SDS surfactants on mica (so long as there are no cross-linking divalent cations present such as Ca^{+}).
(28) Taunton, H. J.; Toprakcioglu, C.; Fetters, L. J.; Klein, J. *Macromolecules* **1990**, *23*, 571.
(29) Marra, J.; Israelachvili, J. N. *Biochemistry* **1985**, *24*, 4608.
(30) Luckham, P. F.; Klein, J. *J. Chem. Soc., Faraday Trans.* **1984**, *1*, 865.
(31) See ref 17 and other references therein.